

REPORT DOCUMENTATION PAGE				Form Approved OMB No. 0704-0188	
<p>The public reporting burden for this collection of information is estimated to average 1 hour per response, including the time for reviewing instructions, searching existing data sources, gathering and maintaining the data needed, and completing and reviewing the collection of information. Send comments regarding this burden estimate or any other aspect of this collection of information, including suggestions for reducing the burden, to the Department of Defense, Executive Service Directorate (0704-0188). Respondents should be aware that notwithstanding any other provision of law, no person shall be subject to any penalty for failing to comply with a collection of information if it does not display a currently valid OMB control number.</p> <p>PLEASE DO NOT RETURN YOUR FORM TO THE ABOVE ORGANIZATION.</p>					
1. REPORT DATE (DD-MM-YYYY) 23/04/2012		2. REPORT TYPE Final Report		3. DATES COVERED (From - To) October 1, 2008 - March 31, 2012	
4. TITLE AND SUBTITLE High-Temperature Spintronic Devices and Circuits in Absence of Magnetic Field			5a. CONTRACT NUMBER N00014-09-1-0086		
			5b. GRANT NUMBER F021874		
			5c. PROGRAM ELEMENT NUMBER		
6. AUTHOR(S) Pallab Bhattacharya, University of Michigan Supriyo Datta, Purdue University			5d. PROJECT NUMBER 09PRO1990-01		
			5e. TASK NUMBER		
			5f. WORK UNIT NUMBER		
7. PERFORMING ORGANIZATION NAME(S) AND ADDRESS(ES) University of Michigan, Electrical Engineering and Computer Science; 1301 Beal Avenue; #2306 EECS, Ann Arbor, MI 48109-2122 Purdue University, School of Electrical and Computer Engineering; West Lafayette, IN 47907				8. PERFORMING ORGANIZATION REPORT NUMBER 06239	
9. SPONSORING/MONITORING AGENCY NAME(S) AND ADDRESS(ES) Office of Naval Research 875 N. Randolph Street, #1425 Arlington, VA 22203-1995				10. SPONSOR/MONITOR'S ACRONYM(S)	
				11. SPONSOR/MONITOR'S REPORT NUMBER(S)	
12. DISTRIBUTION/AVAILABILITY STATEMENT Unlimited					
13. SUPPLEMENTARY NOTES					
14. ABSTRACT <p>The main object of this project was to demonstrate: (a) spin-polarized light sources with large output circular polarization, and (b) spin-based electrical devices that could be ultimately applicable for logic and memory applications operating at high temperatures and in the absence of an externally applied magnetic field. For electrical spin-based devices, our focus shifted to multi-terminal spin valves in the vertical configuration as opposed to the lateral configuration. The long-term goal of this project was to study and gauge the prospects of engineering practical high temperature opto- and electrical semiconductor-based spintronic devices.</p>					
15. SUBJECT TERMS Optoelectronics, Memory Devices, Data Processing					
16. SECURITY CLASSIFICATION OF:			17. LIMITATION OF ABSTRACT	18. NUMBER OF PAGES	19a. NAME OF RESPONSIBLE PERSON
a. REPORT	b. ABSTRACT	c. THIS PAGE			19b. TELEPHONE NUMBER (Include area code)
U	U	U	UU	13	

**High Temperature Spintronic Devices and Circuits
In Absence of Magnetic Field**

Principal Investigator

Pallab Bhattacharya

1301 Beal Ave., EECS 2306, Ann Arbor, MI

Phone: 734-763-6678

Fax: 734-763-9324

E-mail: pkb@eecs.umich.edu

Co-Principal Investigator

Supriyo Datta

465 Northwestern Ave., West Lafayette, Indiana

Phone: Fax: 765-494-3511

Fax: 765-494-2706

E-mail: data@ecn.purdue.edu

Submitted to Office of Naval Research

875 North Randolph Street, Suite 1245, Arlington, VA 22203-1995

Attn: Dr. Chagaan Baatar

April 2012

High-Temperature Spintronic Devices and Circuits in Absence of Magnetic Field

P.I.: Professor Pallab Bhattacharya

Electrical Engineering and Computer Science
University of Michigan
Ann Arbor, MI 48109

phone: (734) 763-6678 fax: (734) 763-9324 email: pkb@eecs.umich.edu

Co-P.I.: Professor Supriyo Datta

School of Electrical and Computer Engineering
Purdue University
West Lafayette, IN 47907

phone: (765) 494-3511 fax: (765) 496-6026 email: datta@purdue.edu

Award Number: N00014-09-1-0086

OBJECTIVES

The main object of this project was to demonstrate: (a) spin-polarized light sources with large output circular polarization, and (b) spin-based electrical devices that could be ultimately applicable for logic and memory applications operating at high temperatures and in the absence of an externally applied magnetic field. For electrical spin-based devices, our focus shifted to multi-terminal spin valves in the *vertical* configuration as opposed to the *lateral* configuration. The long-term goal of this project was to study and gauge the prospects of engineering *practical* high temperature opto- and electrical semiconductor-based spintronic devices.

APPROACH

Our technical approach includes growth, fabrication, and analysis of spin-based optical and electrical devices. Some of the key approaches employed are:

- Theoretical simulation of spin transport in semiconducting materials using the non-equilibrium Green's function (NEGF) formalism.
- Molecular beam epitaxy (MBE) growth of ferromagnetic metals (Fe, MnAs) and semiconductor/ferromagnet heterostructures
 - Low-temperature epitaxy of device-quality GaAs on MnAs
 - SQUID (superconducting quantum interference) and MOKE (magneto-optical Kerr effect) measurements for characterization of ferromagnets.
- Characterization (dc, polarization, polarization modulation) of spin VCSELs.
- Magnetic field dependent local, non-local, and Hanle measurements on semiconductor lateral and vertical spin valves.
- Electrical characterization of multi-terminal spin devices as a function of temperature.

Key Individuals that participated in this project are:

Prof. Pallab Bhattacharya, Hyun Kum, Debashish Basu, and Dipankar Saha from the University of Michigan-Ann Arbor.

Prof. Supriyo Datta, Abu Naser Zainnudin, Lufte Siddiqui, and Kerem Camsari from Purdue University.

WORK COMPLETED

Major technical accomplishments achieved in this project are:

1. Demonstration of laser output polarization of a spin laser, up to 100%, independent of spin injection and magnetization of spin contact.
2. Experimental demonstration of an electrically injected quantum dot spin polarized single photon source.
3. A vertical GaAs/MnAs spin valve with high magnetoresistance at room temperature.
4. Amplification of magnetoresistance (~600%) at room temperature, in a three-terminal vertical spin device.
5. Electric field control of magnetoresistance in a lateral 2DEG InAs quantum well spin valve.
6. Theoretical model and experimental verification on mesa size dependence of magnetoresistance in lateral semiconductor spin valves

RESULTS

A summary of significant results, conclusions, and a discussion of each technical accomplishment is described in the following sections.

1. *Electrical Field Modulation of Spin Transport*

Electrical spin injection, manipulation, transport and detection in non-magnetic semiconductors have been demonstrated in several spin based electronic and optoelectronic devices. However, the electrical control of spin transport with a gate-like electrode in a spin valve or lateral magnetoresistance device has proven to be more difficult. This is mainly because of the difficulty in bringing together a channel material with optimal spin-related characteristics with efficient analyzer, polarizer and gate electrodes. In the present study we have investigated the modulation of lateral spin transport in an InAs/In_{0.53}Ga_{0.47}As modulation doped heterostructure lattice-matched to InP with a gate electrode. The electrical control of the magnetoresistance in conventional spin valves is unambiguously observed. We have compared our results with those obtained from an identical GaAs channel spin valve, for which no modulation of the magnetoresistance with gate voltage is observed. This confirms that the observed effects in the InAs quantum well spin valves arise from Rashba spin-orbit coupling. *This experiment demonstrates, for the first time, the capability to manipulate the spin of electrons via an applied electrical field.*

Modulation-doped InAs/In_{0.53}Ga_{0.47}As/In_{0.52}Al_{0.48}As heterostructure was chosen as the active channel of the spin valve since the reported modulation of the Rashba coefficient by a gate bias in an InAs/In_{0.53}Ga_{0.47}As/In_{0.52}Al_{0.48}As heterostructure is relatively large compared to that in bulk GaAs. The ferromagnetic polarizer and analyzer contacts are realized with 35 nm type-B MnAs grown at 250 °C on 30 nm n-doped (graded) In_{0.52}Al_{0.48}As to form Schottky tunnel barriers. The devices are fabricated by using standard optical lithography, metallization, plasma enhanced chemical vapor deposition (PECVD) and e-beam evaporation techniques.

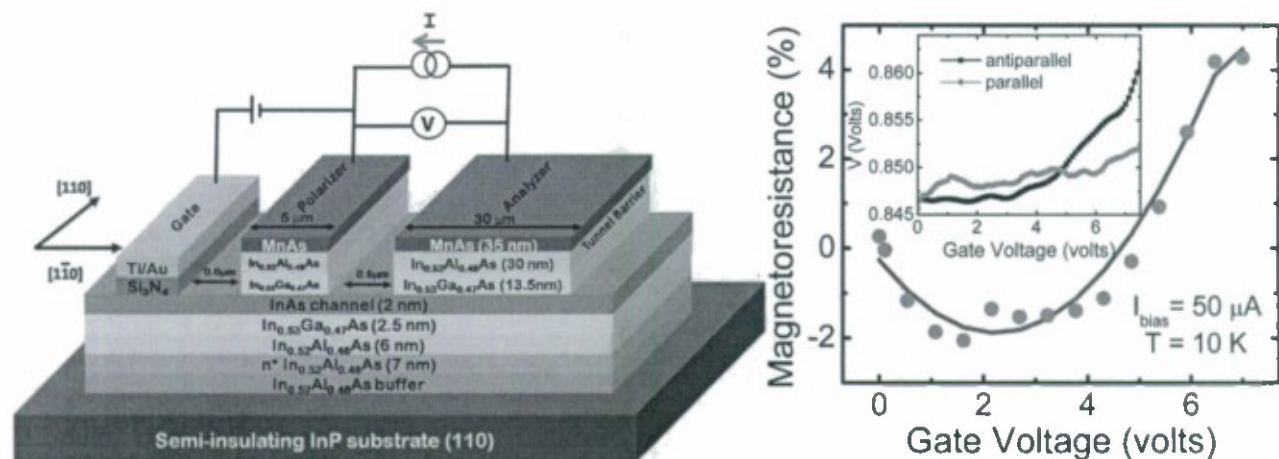


Figure 1. (left) Schematic illustration of the heterostructure and biasing scheme used in this experiment. (right) Modulation of magnetoresistance as a function of applied gate voltage.

The devices were mounted in a liquid helium cryostat for measurements, with provisions for the application of a magnetic field along the easy axis of the MnAs contacts. The device operates as a conventional lateral spin valve and the measured magnetoresistance $MR(H) = [R_{\uparrow\downarrow}(H) - R_{\uparrow\uparrow}(H_{sat})]/R_{\uparrow\uparrow}(H_{sat})$ is a manifestation of the polarizer and analyzer efficiencies changing by different amounts with changing magnetic field, by virtue of their different coercivities. The variation of peak magnetoresistance versus bias current data indicates an almost negligible decrease of magnetoresistance with bias current. The observed behavior is the result of two competing effects: increased spin dephasing due to Dresselhaus and enhanced Rashba spin orbit coupling terms at high electron densities, which will lead to a decrease in injected spin polarization, and a decrease in the polarizer depletion region width with increasing current bias, which will lead to more efficient tunneling and injection of spin polarized carriers.

The voltage V between the polarizer and analyzer terminals is measured at 10K and 20K for as a function of bias applied to the insulated gate, V_G , for both parallel and antiparallel magnetization of the MnAs pads. The measurement is done at a constant injection current of 100 μA and with no externally applied magnetic field. An oscillation of magnetoresistance as a function of gate voltage is observed. The oscillation is a result of the cross-over in the parallel and anti-parallel voltages, which is due to the spin precession of injected carriers. Identical data were recorded with a constant injection current of 150 μA between the polarizer and analyzer. The experiment was repeated with two control devices, in both of which the channel length is 150 μm and in one of them the analyzer is a non-magnetic Ti/Au contact. All other dimensions are maintained the same. For both of these devices, the variation of V with V_G for parallel and antiparallel magnetization of the polarizer and analyzer does not exhibit any cross over. As a consequence no oscillation of the magnetoresistance as a function of gate voltage is recorded. The oscillation in the magnetoresistance is a manifestation of spin dephasing of the injected electrons and is an indication of the modulation of spin transport by an applied electric field.

The fact that the magnetoresistance can be modulated even in a device with large polarizer/analyzer contact dimensions and channel length is very encouraging. By shrinking these dimensions considerably to submicron and nanometer scales, the adjacent gate can easily induce an electric field in the channel region and these devices can be operated at higher temperatures and higher frequencies. These results indicate that the change in magnetoresistance is caused, in part, by Rashba

spin-orbit coupling due to the gate bias. While this demonstration together with the recently reported work are very encouraging, further work is necessary before any claims to practical room-temperature applications can be made.

2. Room Temperature Lateral Spin Valves

As a first step towards the realization of practical high temperature spintronic devices we have investigated the characteristics of conventional spin valves with nanometer channel lengths, fabricated on a GaAs substrate. Lateral conventional spin valves with channel lengths $L_{\text{chan}} \sim 42$ nm with polarizer (P) and analyzer (A) contact length-to-width aspect ratios (L/W) of 10 and 1.5 respectively, were fabricated using conventional wet, dry and focused ion beam etching, photolithography, and metallization techniques. MnAs ferromagnetic layers were used as spin injector and detector electrodes. Graded doped Schottky tunnel barriers were used to efficiently inject spin from MnAs into the GaAs channel. The magnetoresistance, defined as $MR(H) = [R_{\uparrow\uparrow}(H_{\text{sat}}) - R_{\uparrow\downarrow}(H)] / R_{\uparrow\uparrow}(H_{\text{sat}})$, of the spin valves were measured for various temperatures (T), and bias conditions (I_B). The MR for the device peaks at 0.5% for $|H| \sim 1000$ Oe in both directions of the magnetic field sweep at $T = 298$ K. The MR peaks correspond to antiparallel magnetization of the MnAs pads arising from their coercive field difference. Spin valves across various grown and processed samples with $L_{\text{chan}} = 42$ nm were measured under identical experimental conditions, and the results are highly reproducible. This experiment conclusively proves the diffusive nature of spin transport in a semiconductor material, and is highly dependent on temperature. From these results, one can conclude that higher temperature leads to an increase in spin relaxation rate, leading to shorter spin lifetimes and, thus, shorter spin diffusion lengths.

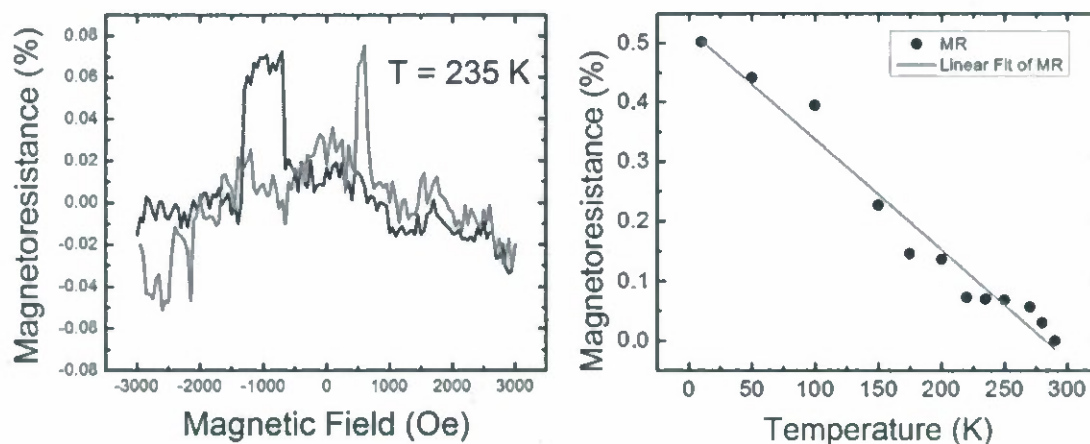


Figure 2. (left) Magnetoresistance characteristics of a high temperature spin valve at $T = 235$ K. (right) Magnetoresistance response as a function of temperature. Clear MR signal is observed at 300 K.

3. An electrically injected quantum dot spin polarized single photon source

A source of single photons with controlled polarization, circular or linear, would be very useful for quantum cryptography. In single photon sources employing microcavities, this can be implemented by engineering emission preferentially into a given polarization mode, or by engineered asymmetry in the cavity or reflector. A more direct and elegant technique would be to inject spin polarized carriers into the active region. Upon radiative recombination of these carriers, their angular momentum is transferred to photons due to well known selection rules, generating circularly polarized light. We have experimentally investigated the output polarization characteristics of an electrically injected spin

polarized single photon source in which the photons are emitted from a single InAs quantum dot embedded in a GaAs microcavity. It is seen that the nature of the output polarization, circular or linear, can be varied by varying a transverse magnetic field.

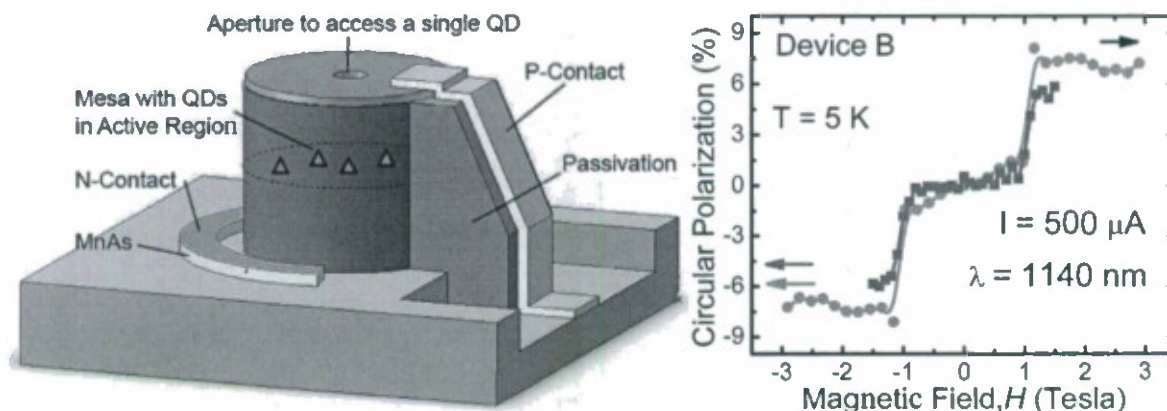


Figure 3. (left) Illustration of the single photon source with MnAs ferromagnetic n-contact. (right) Net output circular polarization vs. magnetic field measured for two diode injection currents in the Faraday geometry.

The quantum dot microcavity device was grown by molecular beam epitaxy with a low dot density (verified by atomic force microscopy). Mesa-shaped devices ($40\text{ }\mu\text{m}$ diameter) were fabricated by standard lithography, wet and dry etching and contact metallization. Spin polarized electrons are injected via a selectively regrown MnAs/ $n^+\text{Al}_{0.1}\text{Ga}_{0.9}\text{As}$ Schottky barrier heterostructure. A small aperture, $0.6\text{ }\mu\text{m}$ in diameter, is formed in the top 75 nm thick Al layer such that light from a single dot below the aperture is emitted through it. Single photon emission from the device was confirmed by measuring the photon pair correlation statistics of the electroluminescence with a Hanbury-Brown and Twiss arrangement. The intensity and polarization characteristics of the biexciton photons from the InAs quantum dot were measured at 5 K by mounting the device in a magneto-optical cryostat. The measurements are made in the Faraday geometry in which the magnetic field is applied in the direction of photon emission. The MnAs spin injector is therefore magnetized along the hard axis of magnetization. Measurements are done with the applied magnetic field varying in the range $0\text{--}1.4\text{ T}$ in the wavelength range of the biexciton emission, to take advantage of the higher emission intensity, for a fixed injection current of $500\text{ }\mu\text{A}$. It is observed that up to a magnetic field of 0.9 T , the photons are predominantly linearly polarized and for higher fields the photons are circularly polarized. The output circular polarization remains zero upto a magnetic field of 0.9 T , beyond which point it increases to a saturation value. The intensity of the emission remains constant with magnetic field. The output polarization characteristics of the control device are very different. No net circular polarization is observed at zero or any applied magnetic field upto 2 T . Instead, the output exhibits linear polarization which decays to zero at 1 T . The measured degree of circular polarization is determined by the magnetization of the contact, its injection efficiency and the transport characteristics of the spin-polarized electrons from the MnAs contact to the active quantum dot. With enhanced output circular polarization, the device described here could be useful for polarization encoded cryptography, where the train of emitted single photons would have a preferred polarization instead of random polarization. The output polarization can be linear at $B = 0$, or circular for $B \geq 1\text{ T}$.

4. High-frequency dynamics of spin-polarized carriers and photons in a laser

There is a dynamic exchange of energy between carriers—electrons and holes—and photons in a resonant cavity whenever the carrier population is perturbed by external means. The latter can be in

the form of electrical injection or optical excitation. Thus, in a semiconductor laser cavity a damped oscillatory optical output is observed. This is accompanied by a similar perturbation in the carrier density, usually of smaller amplitude. The system behaves as a tuned circuit and a resonant condition can be achieved in the system transfer function, which is the ratio of the light output to the injected carrier density, at some characteristic oscillation frequency. These relaxation oscillations, which exist for several nanoseconds and are related to the spontaneous emission lifetime, set an upper limit to the modulation frequency of a laser. In fact, the frequency of the relaxation oscillations at the tail end, where small-signal conditions are prevalent, approximates the resonant frequency for small signal modulation of the laser. It is generally understood that a laser restores steady state in the duration of the oscillations. In a semiconductor laser, relaxation oscillations give rise to deleterious effects such as linewidth enhancement and chirp due to the periodic modification of the refractive index in the active gain region by the carrier concentration modulation. The spin polarization of recombining electrons and holes generally do not play a role in the operation of a conventional laser. Radiative recombination of spin-up and spin-down carriers in the active region of any semiconductor light source produces left- and right-circularly polarized light, respectively. In a conventional laser, these two polarization modes are pumped equally, from equal injection of spin-up and spin-down carriers. The two equal and in-phase circularly polarized modes combine to form linearly polarized emission. Preferential injection of spin-polarized carriers lead to emission of circularly or elliptically polarized light via the selection rules for radiative recombination. While the steady-state characteristics of optically and electrically injected spin-polarized laser have been studied in detail, by theory and experiment, the effect of a net spin polarization of carriers in the active region on the dynamic or transient, properties have not been fully examined, or exploited.

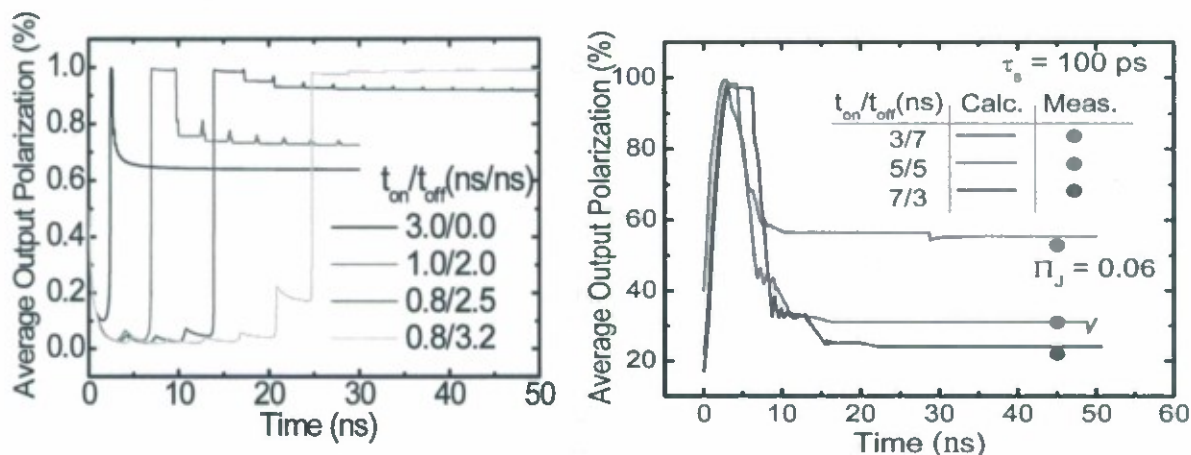


Figure 4. (left) Time-averaged output circular polarization as a function of time for various t_{on} and t_{off} of an ideal square pulse bias with zero rise and fall times. (right) Output polarization calculated and measured for a spin laser with a pulse current bias having finite identical rise and fall times.

A theoretical study of the small-signal modulation properties of the dominant or favored circularly polarized mode of a spin laser was recently reported, from which it is evident that the modulation bandwidth is enhanced. This is understood since a spin laser attains threshold with a smaller density of injected carriers. Of practical importance and interest are the large-signal modulation characteristics of the spin laser, the temporal evolution of the relaxation oscillations of *both* polarization modes and the temporal evolution of the net output polarization. In this work we have examined the role of injected carriers with a net spin polarization on the large- and small-signal modulation characteristics of a semiconductor laser. In particular, we have investigated the region of

operation near threshold of the laser, where large gain anisotropy of the two polarization modes exists. The calculated transient characteristics clearly show temporally separated relaxation oscillations for the two polarization modes and predict an increase in the small signal modulation bandwidth. *The simulations also predict that an output circular polarization of 100% can be obtained, under certain biasing conditions, irrespective of the spin polarization of the injected carriers.* This fact is of great practical importance since the spin polarization of injected carriers in the active region of a spin laser at high temperatures is usually in the range of 5–6 %. However, it may be noted that very low values of injected spin polarization reduce the flexibility in biasing conditions required to achieve high output circular polarization. We have experimentally verified this phenomena by performing measurements on a InAs/GaAs quantum dot (QD) vertical cavity surface emitting laser (VCSEL) in which spin-polarized electrons are injected into the quantum dots by a MnAs ferromagnetic contact. The spin VCSEL operates at 230 K and a maximum output polarization of 55% is measured. These characteristics make a spin laser a very practical and useful device for a host of applications including study of biological structures, fibrous proteins and pharmacological properties of drugs, reconfigurable optical interconnects, and secure communication.

5. Gate Control and Amplification of Magnetoresistance in a Three-terminal Vertical Device

The overriding goal of the emerging field of spintronics is to develop devices that integrate charge and spin properties of semiconductors to achieve non-volatility, higher processing speeds, higher packing densities, and reduced power consumption. Two fundamental requirements for the realization of successful spintronic devices are the generation and control of spin currents in a non-magnetic semiconductor. It is essential to be able to amplify the magnetoresistive effect by controlling the flow of spin polarized carriers in a conventional spin valve. *In this work, we developed a new device – a GaAs/MnAs vertical spin valve with a third gate terminal – and produced ~500% modulation of the magnetoresistance at room temperature.* The device is produced by a single epitaxial growth step and subsequent processing. The gate terminal effectively shifts the band energy in the GaAs channel and thereby changes spin injection, transport, and detection. The modulation of magnetoresistance has been analyzed by a model based on one-dimensional (1D) spin drift-diffusion and the voltage dependence of tunneling resistance at the tunnel injector contacts. The device can be used as a non-volatile magnetic memory and can be integrated with microelectronics circuits.

Fully epitaxial vertical spin valve heterostructures consisting of MnAs (35 nm) / undoped-GaAs (0.5 nm) / undoped-AlAs tunnel barrier (1 nm) / p+-GaAs channel (10 nm, 1×10^{19} Mn-doped) / undoped-AlAs (1 nm) tunnel barrier / undoped-GaAs (0.5 nm) / MnAs (25 nm) were grown by molecular beam epitaxy (MBE) on semi-insulating GaAs (100) substrate. The heterostructure was grown at a substrate temperature of 250 °C for the bottom MnAs layer, and 200 °C for subsequent layers to avoid interlayer diffusion of Mn atoms and formation of Mn-Mn clusters. The Mn atoms allow low temperature p-doping of GaAs without affecting the MnAs/GaAs interface, which is otherwise difficult to achieve. The 0.5 nm GaAs layers are grown to provide a smooth surface for growth of successive layers and to prevent interdiffusion between AlAs and MnAs. It may be noted that besides acting as a tunnel barrier for efficient spin injection and detection, the AlAs layers also prevent segregation of Mn atoms at the MnAs/GaAs:Mn interface. Standard optical lithography was used to fabricate the devices in circular mesas. Besides the two ferromagnetic type-A MnAs spin injector and detector electrodes, a third “gate” electrode (Ti/Au) was deposited on top of the heavily p-doped GaAs semiconducting channel layer via e-beam assisted evaporation and lift-off.

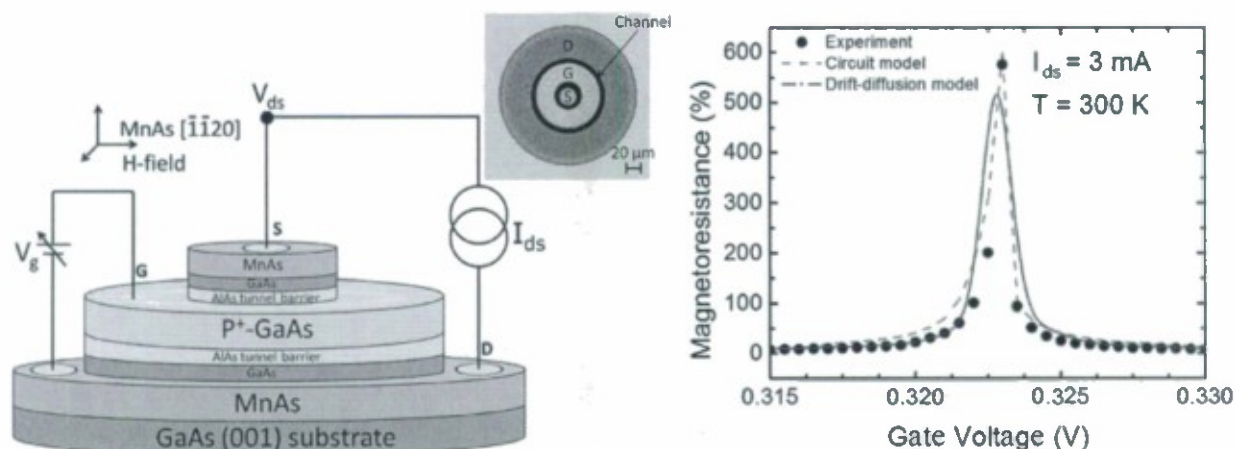


Figure 5. (left) Illustration of the geometry, heterostructure, and measurement scheme used for the three terminal magnetoresistance amplifier. (right) Amplification of magnetoresistance with applied gate voltage at 300 K.

Magnetoresistance (MR) measurements were made with the devices in a closed-loop He cryostat placed between the poles of an electromagnet. The magnetic field is applied in-plane along the easy axis of MnAs [1120]. Measurements were first made with no bias (gate floating) applied to the gate (third) terminal, the device thereby behaving as a vertical spin valve. A constant dc bias current (I_{ds}) is applied between the two MnAs contact layers (source and drain) and the voltage V_{ds} is measured between the same terminals while varying the applied magnetic field. The magnetoresistance is calculated as $MR = (V_{AP} - V_P) / V_P$, where V_P and V_{AP} are the measured terminal voltage V_{ds} for parallel and anti-parallel alignment of the two MnAs contacts. With optimized device design and epitaxial growth of the ferromagnet-semiconductor heterostructure, we are able to achieve a value of $MR \approx 27\%$ which is amongst the largest reported in any semiconductor spin valve at room temperature. No magnetoresistance was observed in control devices with (a) channel thickness much greater than the spin diffusion length and (b) the top MnAs contact replaced by a non-ferromagnetic Ti/Au contact.

The results of three-terminal measurements, with the application of a gate bias, are described next. A constant current bias I_{ds} is applied between the two MnAs contacts and a voltage V_g is applied to the gate terminal. The two MnAs contacts are successively set in parallel and anti-parallel magnetization with the application of appropriate magnetic fields (depending on the individual coercivities of the contacts) and in each case $V_{ds} = V_P$ or V_{AP} is measured as the gate bias is varied. The control and amplification of magnetoresistance with the gate terminal is evident, where the values of MR reach as high as 600% at room temperature.

With an applied current bias, spin polarized electrons injected by the source MnAs/AlAs/GaAs tunnel barrier are transported across empty valence band states at the Fermi energy in the GaAs channel and are collected at the drain ferromagnet-semiconductor Schottky tunnel contact. At the same time, the band bending in the semiconductor changes, mostly at the drain end, accompanied by a change in width and height of the drain Schottky tunnel barrier. In effect, the interface resistance and spin selectivity of the tunnel contacts are modulated. Additionally, at high values of applied bias, unpolarized electrons from filled valence band states below the Fermi level in GaAs can tunnel into the MnAs contact layer and result in a component of unpolarized current. The bias dependence of magnetoresistance due to the changes in the bands and contacts is analyzed by describing spin transport with the drift-diffusion model of Valet and Fert, and Yu and Flatté. Tunneling across the source and drain Schottky barriers is analyzed with the Tsu-Esaki model using the WKB

approximation and assuming that there is no spin scattering at the ferromagnet-semiconductor interfaces. Thus, the bias dependence of the tunneling resistance and the MR of the device are obtained. The calculated variation of MR with bias in the two-terminal spin valve is calculated and the agreement is very good with measured data.

The observed variation and amplification of MR with V_g is a result of the change in the effective bias applied between the two MnAs Schottky tunnel contacts, which change the band bending in GaAs, the tunnel barrier thickness, and the interface resistance and spin selectivity of the tunnel contacts. In effect, the gate terminal modulates the spin current collected at the drain terminal. At a critical gate bias, when the two ferromagnetic electrodes are in the parallel configuration, the voltage drop across the device ($V_{ds\text{-parallel}}$) will be near zero (state 0). When the electrodes are in the antiparallel direction, the voltage drop ($V_{ds\text{-antiparallel}}$) will be some finite value (state 1). The dual state of this device allows it to be a single bit for a storage element, and the state of this device is determined solely by the relative polarization of the injector/detector ferromagnetic electrodes. Although a magnetic tip would be required for MnAs based devices to switch the device from either parallel or antiparallel state, several ferromagnets exhibit electrical control of magnetism which could be utilized to create an all electrical non-volatile spin memory arrays that are reconfigurable and monolithically integrated with CMOS logic devices.

6. Mesa size dependence of magnetoresistance in lateral semiconductor spin valves

Lateral spin valve devices with semiconducting channels have the potential for use in future spin-based information process technology. However spin injection and detection processes are still very inefficient in these devices. For example, in a two terminal local measurement setup the magnetoresistance (MR) values achieved to date are far smaller than the maximum limit of $p^2/(1-p^2)$, p being the spin-injection or detection efficiency. In such devices, it has already been discussed that reducing the distance between the injector and detector pad shorter than the spin-diffusion length (λ_s) will reduce spin-relaxation in the current path leading to an increase of MR. However this criterion by itself will not achieve the maximum MR. Channel regions outside the current path, which usually remain unetched, may also act as a source of spin-relaxation and significantly decrease the MR response and forms the subject-matter of this study. *This work serves a three-fold purpose: 1) it introduces a compact circuit-level description of spin transport that is derived from a one dimensional spin-diffusion equation and thus, enables circuit-level insights to assist the optimization of local two probe lateral spin-valve devices, 2) it provides an analytical expression for MR, derived from the mentioned circuit model, when the channel length is smaller than spin-diffusion length and identifies the parameters which are responsible for reducing the MR in such a case and describes the conditions under which an extended mesa region beyond the ferromagnetic contacts significantly reduces the MR and finally, 3) it provides preliminary experimental data that seems to support the conclusions.*

Spin transport in lateral spin valves are usually described by the spin diffusion equation which is valid in the limit where spin-diffusion length is larger than the mean free path. Including an interfacial conductance to account for the ferromagnet-tunnel barrier (FM-TB) the spin-diffusion equation can be written as (V : applied bias),

$$\begin{aligned} \frac{d^2 \mu_x^{+-}}{dx^2} &= (\mu_x^{+-} - \mu_x^{-+}) / 2\lambda_s^2 + 2r_{sc} g_c^{+-} (\mu_x^{+-} - V), \text{ under contacts} \\ &= (\mu_x^{+-} - \mu_x^{-+}) / 2\lambda_s^2, \text{ elsewhere} \end{aligned} \quad (1)$$

where μ_x^{+-} is the spin-dependent electrochemical potential along the transport direction (x) for majority (+) and minority (-) spins. r_{sc} is the sheet resistance of the semiconducting channel in Ω/m . g_c^+ and g_c^- are the spin dependent interfacial conductances of FM-TB contacts in $m^{-1}\Omega^{-1}$ for '+' and '-' spins, respectively. To solve Equation 1 we assumed that at two edges of the channel $d\mu^+/dx = d\mu^-/dx = 0$, which implies that there is no spin-relaxation at the edges. Equation 1 can be pictorially represented by a distributed network of series and shunt resistance components (see Figure 1(c)). Kirchhoff's current conservation law applied at each node of this distributed circuit will yield a set of equations that is identical to a discretized version of Equation 1. The components are given by, $[G_c] = [g_c^+ 0; 0 g_c^-]$, $[R_{sc}] = [2r_{sc} 0; 0 2r_{sc}]$ and $[G_{sf}] = [g_s -g_s; -g_s g_s]$. Here, g_s is the spin-relaxation conductance ($m^{-1}\Omega^{-1}$) connecting both spin channels, and is given by $1/(4r_{sc}\lambda_s^2)$.

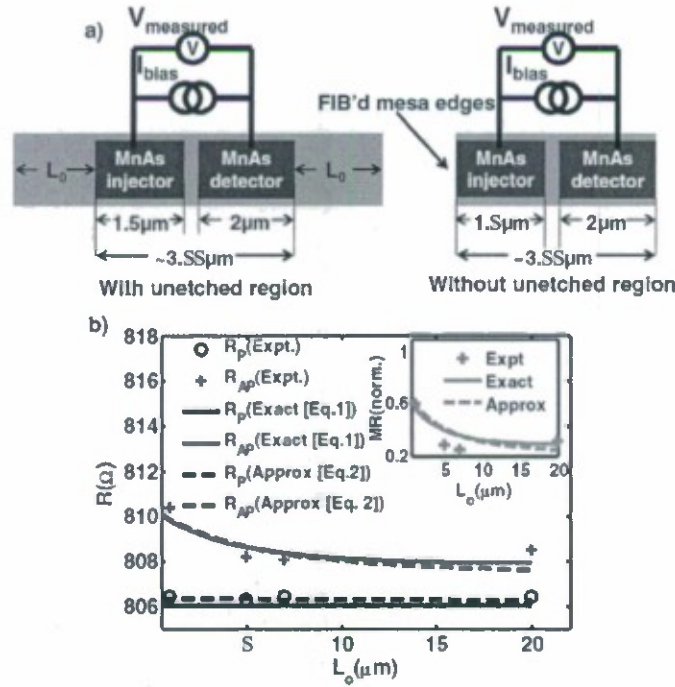


Figure 6. (a) Local measurement scheme of a device with unetched and etched mesa. (b) Parallel and anti-parallel resistances of the spin valves as a function of unetched mesa length.

The distributed network can be replaced by an equivalent lumped (l) network, by approximating the extended contacts with point source contacts but keeping the total conductance the same. Such an approximation is valid when spin polarized electrons can easily penetrate underneath the contacts with negligible lowering of their chemical potential, which implies that the contact lengths are far smaller than the charge penetration depth as well as the spin-diffusion length. As a result, in the lumped network, $g_c^+ \rightarrow g_c^{+,o}$ ($m^{-1}\Omega^{-1}$) $\times L_c$ inside $[G_c]_l$, where L_c is the contact length. The series $[R_{sc}]$ components can be replaced with a single $[R_{sc}]_l$ given by $[R_{sc}]_l = [r(1+a) r(1-a); r(1-a) r(1+a)]$, where L_l is the channel length inside the current path, $r = r_{sc}L_l$, and $a = (\lambda_s/L_l)\sinh(L_l/\lambda_s)$. The shunt spin-relaxation components are separated into two spin-relaxation components, one for channel regions in the current path ($[G_{sf}^i]_l$) and another for channel regions out of the current path ($[G_{sf}^o]_l$), given as, $[G_{sf}^i]_l = [g_s^{i,o} -g_s^{i,o}; -g_s^{i,o} g_s^{i,o}]$ where $g_s^{i,o} = 1/(2r_{sc}\lambda_s)\tanh(L_{l,o}/2\lambda_s)$. We note that since there is no

charge current flowing in the unetched regions, the spin components of the charge current would be equal in magnitude but opposite in direction and, thereby, resulting in a shunt spin-relaxing path g_s^o . By solving the lumped network for parallel (R_p) and anti-parallel (R_{ap}) resistances, we can write an expression for MR as (assuming $L_i \ll \lambda_s$),

$$\begin{aligned}
 R_p &= \frac{2}{g_c} \left[\frac{y^2 \{4x + (1-p^2)\} + 2y(1+2x) + 1}{1 + y \{4x + (1-p^2)\}} \right] \\
 R_{ap} &= \frac{2}{g_c} \left[\frac{(1+4x)}{\{4x + (1-p^2)\}} + y \right] \\
 MR &= \frac{R_{ap} - R_p}{R_p} = \frac{p^2}{[1 + 4xy + y(1-p^2)][1 + 4xy + y(1-p^2) + 4x] - p^2} \\
 p &= \frac{g_c^+ - g_c^-}{g_c}, g_c = g_c^+ + g_c^-, x = \frac{g_s^i + g_s^o}{g_c} = \frac{g_{sf}}{g_c}, y = \frac{1}{2} r g_c
 \end{aligned} \tag{2}$$

The MR expression in Equation 2 has two parameters, x and y . In the simplest case where the spin-relaxation conductance (g_{sf}) in the channel and the resistance inside the current path (r) are negligible (i.e. $x \rightarrow 0$ and $y \rightarrow 0$), MR approaches the maximum value of $p^2/(1-p^2)$. Therefore, keeping both x and y as small as possible will lead to a higher MR response. But to stress on the effect of extended mesa we now focus on x and its role on MR assuming y is made sufficiently small by reducing the distance of current path, L_i . However we note that this could as well reduce x but it is not the only factor affecting x . A shorter L_i will reduce the x parameter inside the current path (i.e. $x^i = g_s^i/g_c$), but the component outside the current path ($x^o = g_s^o/g_c$) could still limit MR. So, x^o should also be reduced. This can be done either by etching away the mesa (reducing g_s^o), or by increasing the interface conductance (increasing g_c) for a given mesa length L_o .

To verify the dependence of MR with unetched regions outside the current path, multiple two-terminal spin valves with varying mesa sizes were fabricated on a semi-insulating GaAs substrate with MnAs as the spin injector/detector. The unetched mesa length, L_o and the channel length (<100 nm) for each of these devices were precisely defined by using the focused-ion-beam (FIB) technique. In the supplementary information S1 and S3 we provided a side view of one of these devices along with an SEM image of the edge cut by FIB technique. A standard two terminal local MR measurement was performed as a function of unetched mesa length (L_o) for devices with contact length (L_c) of ~ 1.5 μm .

Preliminary experimental R_p and R_{ap} data are shown as a function of L_o under fixed $I_{bias} = 150\mu\text{A}$ in Fig. 6. Here R_{ap} reduces with L_o whereas R_p stays the almost same. In the parallel configuration, g_c^+ and g_c^- form a balanced 'Wheatstone bridge', leading to a negligible loading effect on $V_{measured}$ due to change in g_s^o with L_o . But the anti-parallel configuration creates significant imbalance in the bridge, which drives a shunt current through both g_s^i and g_s^o . So an increase in g_s^o eventually loads down $V_{measured}$. By calculating the slope of $R_{p(ap)}$ with respect to x^o (as $x^o \propto L_o$) from Equation 2, we show that R_{ap} should decay faster than R_p with L_o . The experimental data was compared against the two models presented in this work, by solving Equation 1 numerically and Equation 2 directly. Model parameters such as carrier density n_s and mobility μ are obtained from Hall measurement data. λ_s is used as $6.5\mu\text{m}$ which is consistent with the values obtained for bulk-GaAs previously. Contact conductance of $g_c \sim 4 \times 10^8 \text{ m}^{-1} \Omega^{-1}$ was extracted from R_p data. With these values a reasonable agreement with models to experiment was found for spin-injection efficiency, p of $\sim 9\%$.

In conclusion, a compact model for lateral spin-valve devices with semiconducting channel is provided to assist the optimization of the device performance. The effect of extended channel regions outside the current path is discussed. By deriving a simplified expression for magnetoresistance from a one-dimensional spin-

diffusion equation, we show that this unetched region could behave as an additional spin-relaxation source. The effect of MR on such region is demonstrated experimentally, and shows good agreement with the model derived.

IMPACT/APPLICATIONS

The measurement of the effect of electric field control of magnetoresistance via the spin orbit interaction in conventional spin valves, which has remained elusive for the past 19 years, has been experimentally achieved. Also, several ways to enhance the operating temperature and the magnitude of response in semiconductor spin-devices have been theoretically investigated and experimentally demonstrated. The development of the spin-transistor, which has a much improved speed-power metric, as an alternative to present day silicon based CMOS transistors will lead to faster and cooler microprocessors. A novel three-terminal spin-device—a vertical spin transistor—has been demonstrated and characterized. This device could be cascaded into an array of spin memory circuitry, leading to integration of non-volatile and high density memory with conventional CMOS transistors.

Realization of a spin laser with a high degree of spin polarized light will allow tremendous enhancement in the area of biomedical sensing and quantum telecommunication applications. We have initiated and created a platform for practical high-temperature spintronic devices to develop and mature.

PUBLICATIONS

Journal publications:

1. D. Saha, L. Siddiqui, P. Bhattacharya, S. Datta, D. Basu and M. Holub, "Electrically driven spin dynamics of paramagnetic impurities" *Phys. Rev. Lett.* **100**, 196603 (2008).
2. H. Kum, D. Basu, P. Bhattacharya, and W. Guo, "Electric field control of magnetoresistance in a lateral InAs quantum well spin valve" *Appl. Phys. Lett.* **95**, 212503 (2009).
3. D. Saha, D. Basu, and P. Bhattacharya, "High-frequency dynamics of spin-polarized carriers and photons in a laser" *Phys. Rev. B* **82**, 205309 (2010).
4. D. Basu, H. Kum, P. Bhattacharya, and D. Saha, "Characteristics of a high temperature vertical spin valve" *Appl. Phys. Lett.* **97**, 232505 (2010).
5. L. Siddiqui, ANM Zainuddin, and S. Datta, "Electrically driven magnetization of diluted magnetic semiconductors actuated by the Overhauser effect" *J. Phys. Cond. Matt.* **22**, 216002 (2010).
6. A. N. M Zainuddin, H. Kum, D. Basu, S. Srinivasan, L. Siddiqui, P. Bhattacharya, and S. Datta, "Magnetoresistance of lateral semiconductor spin valves" *J. App. Phys.* **108**, 1 (2010).
7. Pallab Bhattacharya, Ayan Das, Debashish Basu, Wei Guo, and Junseok Heo, "An electrically injected quantum dot spin polarized single photon source" *Appl. Phys. Lett.* **96**, 101105 (2010).
8. H. Kum, S. Jahangir, D. Basu, D. Saha, and P. Bhattacharya, "Gate control and amplification of magnetoresistance in a three-terminal device" *Appl. Phys. Lett.* **99**, 152503 (2011).

Conference publications:

1. "High-Temperature Spin-Polarized Lasers With Tunnel Spin Injectors," (INVITED) P. Bhattacharya, D. Basu, M. Holub and D. Saha, *36th Conference on the Physics and Chemistry of Semiconductor Interfaces (PCSI)*, Santa Barbara, CA, January 2009.
2. "Electrically Injected Spin Polarized Lasers," (INVITED), P. Bhattacharya, D. Basu, and D. Saha, *March Meeting of the American Physical Society*, Pittsburgh, PA, March 2009.
3. "Spin Polarized Lasers" (INVITED), P. Bhattacharya, D. Basu, D. Saha and A. Das, *Device Research Conference*, Penn State University, University Park, PA, June 2009.
4. "Spin diffusion in lateral spin valves and spin lasers." (INVITED), D. Basu, P. Bhattacharya and D. Saha, *SPIE Symposium on SPIE NanoScience + Engineering*, San Diego, California, USA August 2009.
5. "Characteristics of an electrically injected single quantum dot spin polarized microcavity light source" (INVITED), A. Das, J. Heo, D. Basu, W. Guo and P. Bhattacharya, *International Symposium on Compound Semiconductor*, University of California, Santa Barbara, 2009.
6. "Electrical control of magnetoresistance in a InP-based lateral spin valve with a two-dimensional electron gas (2-DEG) channel", H. Kum, D. Basu, P. Bhattacharya, and W. Guo, *APS March Meeting*, Portland, Oregon, March 2010.
7. "Output polarization characteristics of an electrically injected quantum dot spin polarized single photon source", A. Das, J. Heo, D. Basu, W. Guo, and P. Bhattacharya, *APS March Meeting*, Portland, Oregon, March 2010.
8. "Properties of MnAs/GaMnAs/MnAs magnetic multilayers and their application to high temperature vertical spin valves", D. Basu, H. Kum, W. Guo, and P. Bhattacharya, *Electronic Materials Conference*, University of Notre Dame, Indiana, 2010.